Evaluation of the Mechanical and Physical Properties of Insulation Fiberboard with Cellulose Nanofibers

Yoichi Kojima Tetsuya Makino Kazuaki Ota
Kazushige Murayama Hikaru Kobori Kenji Aoki
Shigehiko Suzuki Hirokazu Ito

Abstract

The objective of this study was to investigate the lab-scale manufacturing process of insulation fiberboard (IFB) with cellulose nanofibers (CNFs) and evaluate the effects of CNFs on the mechanical and physical properties of the IFB. Because the fabricated IFBs with CNFs had a homogeneous appearance, it was assumed that CNFs can be easily dispersed within IFB by adding them during the mixing stage of the wet process of wood-based board production. The results for the IFBs with CNFs revealed that the density and bending properties increased, while the thickness decreased with an increase in the CNF addition ratio. Furthermore, after the water absorption test, the weight change rates of the IFBs decreased, and the thickness swelling rates increased. Although the size of the specimens was different from the size in JIS A 5905 (Japan Standards Association 2014), the modulus of rupture (MOR) values of IFBs with a target density more than or equal to 0.20 g/cm^3 were higher than the value of A-class IFB in the standard for all CNF addition ratios. In addition, lower thermal conductivity may be realized under similar MOR values by adding CNFs to IFB. On the other hand, to produce CNF-reinforced IFBs with target density/thickness, it is necessary to develop a method for decreasing the cohesive force derived from CNF aggregation and the compressive force originating from the water surface tension caused by the high water retention of CNFs.

Wood-based materials are used extensively in residential construction, particularly in Japan. These materials are made of virgin wood, recycled wood, unused wood species, or thinning wood. Many of the materials are fabricated with adhesives. Most currently available wood adhesives, such as formaldehyde-based resins, vinyl acetate resins, and isocyanate-based resins, are composed of various materials derived from fossil fuels. Synthetic adhesives are usually nonbiodegradable constituents, and they might cause health and environmental problems (Kojima et al. 2016). Thus, the global focus on sustainability demands the development of novel, natural adhesives that do not depend on fossil fuels or synthetic chemicals. Some projects have focused on developing natural, material-based wood adhesives using bioresources. For example, some natural adhesives are composed of citric acid (Umemura et al. 2012a, 2012b, 2012c, 2013; Widodo et al. 2020) or lactic acid (Ikeda et al. 2008, Takatani et al. 2008), but these have not been put to practical use.

In this study, we explored options involving nanofiber technology. Nanotechnology has been developing rapidly in many fields. In general, the term ''nanofiber'' refers to a nanosized fiber and is defined as a fibrous material with a diameter of about 1 to 100 nm and a length more than 100 times the diameter. A fiber that has a surface and inner structure controlled at the nanoscale is called a nanostructured fiber (Kondo 2008). This is true even for fibers that have diameters in excess of 100 nm. Among these nanofibers, cellulose nanofibers (CNFs) have received considerable attention in numerous fields because they are plant-based bioresourced fibers and more than a trillion tons exist worldwide. CNFs also have better physical and

The authors are, respectively, Professor, Former Master Course Student, and Former Master Course Student, Faculty of Agric., Shizuoka Univ., Shizuoka, Japan (kojima.yoichi@shizuoka.ac.jp [corresponding author], makino.tetsuya.15@shizuoka.ac.jp, ota.kazuaki.17@shizuoka.ac.jp); Researcher, Forestry and Forest Products Research Inst., Ibaraki, Japan (kazumura039@ffpri.affrc.go.jp); Assistant Professor and Appointed Professor, Faculty of Agric., Shizuoka Univ., Shizuoka, Japan (kobori.hikaru@shizuoka.ac.jp, kenji.aoki@shizuoka.ac.jp); President, Shizuoka Professional Univ. of Agric., Shizuoka, Japan (suzuki.shigehiko@spua.ac.jp); and Associate Professor, Paper Industry Innovation Center, Ehime Univ., Ehime, Japan (ito.hirokazu.zk@ehime-u.ac.jp). This paper was received for publication in May 2021. Article no. 21-00030.

Forest Prod. J. 71(3):275–282.
doi:10.13073/FPJ-D-21-00030

mechanical properties than most other fibers (Yano 2007). Thus, developing new materials that incorporate CNFs is a high priority (Lee and Ohkita 2003, Nakagaito and Yano 2005, Okubo et al. 2005, Abe et al. 2007, Sehaqui et al. 2011). In our previous reports, the binding effect of CNFs for wood-based boards (i.e., wood flour boards, fiberboards, and particleboards) was investigated (Kojima et al. 2014, 2015, 2016, 2018). The results showed that CNFs have a binding effect for wood-based boards due to three-dimensional binding between the CNFs and wood materials. In these studies, CNF slurry was used as a binder in wood-based boards made by the ''dry process.'' Here, the wooden mats, which were a mixture of wood materials and CNF slurry, had a moisture content greater than 300 percent. This moisture content is much higher than the content of typical wooden mats made by the dry process (about 10%–15%) and is suitable for mats of boards made by the ''wet process.'' Therefore, in this study, we focused on an insulation fiberboard (IFB) made by the wet process. IFB is a low-density fiberboard (density less than 0.35 g/cm^3). It is used for tatami mats and curing boards and as an insulation material. As far as the authors are aware, research on CNF reinforcement of IFBs has not been reported previously.

The wet process of wood-based boards is a process of materials adjustment, wet forming, drying, and finishing, similar to the process of paper production. The effect of CNF reinforcement on paper products has been reported by several researchers. Kawasaki et al. (2017) reported that the air resistance and stiffness of paper were improved by adding TEMPO-oxidized CNFs during the material conditioning (mixing) process. Furthermore, CNFs improved the tensile strength and stiffness of paper produced from a deinked recycled pulp obtained by disintegration and flotation of a mixture of old newspapers and magazines (Delgado-Aguilar et al. 2015). As a result, it is considered that CNFs can be easily dispersed within IFBs during the wet process of wood-based board production and improve the mechanical and physical properties of IFBs because the wet process is similar to the process of making paper.

Therefore, the objective of this study was to investigate the lab-scale manufacturing process of IFB with CNFs and evaluate the effect of CNFs on the physical and mechanical properties of IFBs. This study will contribute to the increase the demand of CNF by investigating the feasibility of CNF as a natural binder for wood-based panel. This study also will contribute to practical use of environmentally friendly thermal insulation material made of biomass.

Materials and Methods

Materials

Softwood (radiata pine) fiber was used as the raw material for the IFB. The average fiber length was 2.27 mm. Commercial CNF slurry (BinFi-s, WFo-10010; Sugino Machine, Uozu City, Japan) consisting of 10 wt% CNFs and 90 wt% water was used in this study.

Fabrication of insulation fiberboards

IFBs with a total of 16 conditions were manufactured under four conditions of target density (0.07, 0.10, 0.20, and 0.30 g/cm^3) and four conditions of the CNF addition ratio (0, 5, 10, and 15 wt%), respectively (Table 1). The CNF addition ratio is a dry basis in this study. The target IFB dimensions were 180 by 180 by 10 mm.

Table 1.—Conditions of fabricating insulation fiberboard with cellulose nanofibers (CNFs).

No.	Target density (g/cm^3)	CNF addition ratio (wt%)
1	0.07	0
2		5
3		10
4		15
5	0.10	0
6		5
7		10
8		15
9	0.20	0
10		5
11		10
12		15
13	0.30	0
14		5
15		10
16		15

Figure 1 shows the experimental procedure used to fabricate the lab-scale IFB with CNFs. First, the amount of wood fibers required for the target board density was measured, and then CNFs were added according to the CNF addition ratio (= CNF solid content/air-dried wood fiber weight), as shown in Table 1. In addition, to form a suspension, water was added until the concentration with respect to the amount of fibers was 1.5 wt%. In the mixing stage, the suspension was stirred for 10 minutes at a rotation speed of 750 rpm using a stirrer. Mixing condition was set to 750 rpm with 10 minutes to refrain from aggregation of wood fiber. Subsequently, in the wet forming stage, Teflon sheets and 100-mesh wire netting were placed beneath the bottom of the forming box (inner diameter of 180 by 180 mm). The suspension was poured into the forming box and allowed to stand. Then the Teflon sheet was pulled out and dehydrated to make a mat. Steel plates with a thickness of 10 mm were placed at both edges of the mat, and the mat was cold-pressed with a desktop press (SA-302; Tester Sangyo Co., Ltd, Tokyo, Japan) at 0.6 MPa for 1 minute. After cold-pressing, the cold-pressed mat was fixed to the steel plates with clamps and then oven-dried at 105°C for 24 hours during the drying stage to complete the IFB. In the drying stage, the completed IFB was stored at a constant temperature of 20°C and relative humidity of 65 percent for more than 3 days. Finally, the conditioned IFBs were cut to sizes appropriate for surface morphology, bending, water absorption, and thermal conductivity tests, and then their physical and mechanical properties were evaluated. The data of physical and mechanical properties were analyzed with two-way analysis of variance to test for significant effects of the CNF addition ratio, target density, and their interaction.

Surface morphology test

The IFB surface was attached to a sample stand and dried at 60°C for 3 days or more with a vacuum constant temperature dryer (VOC0300SD; EEYLA Tokyo Rika Kikai Co., Ltd, Tokyo, Japan). Using an auto fine coater (JEC-3000FC; JEOL Ltd, Tokyo, Japan), the observation surface was coated with platinum with a target film thickness of 5 nm and then observed with a scanning electron microscope (SEM) (JSM-6510LV; JEOL).

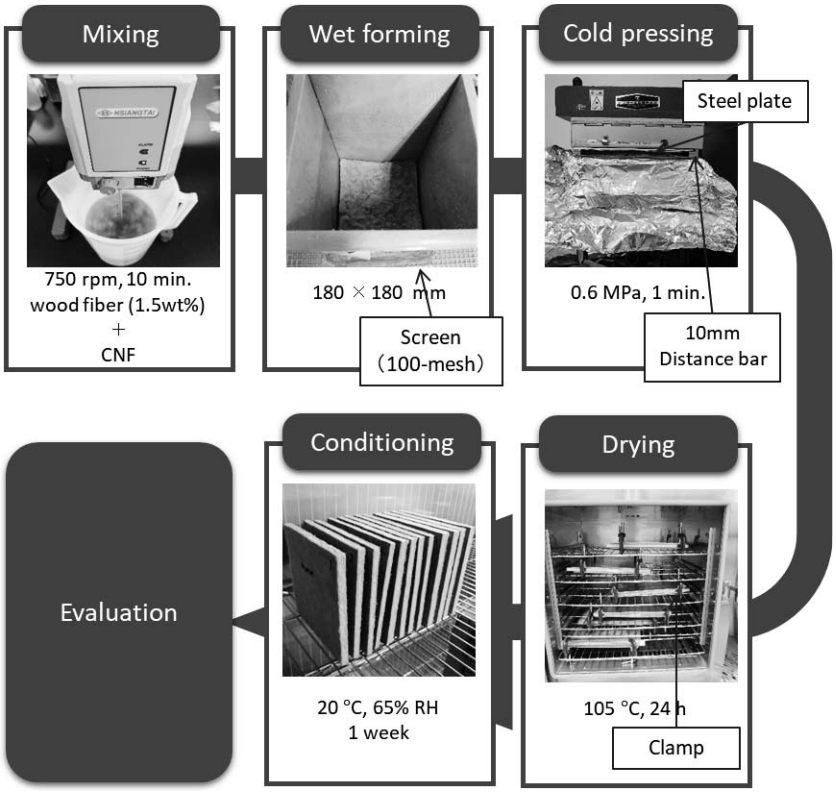

Figure 1.—Experimental procedure used to fabricate the lab-scale insulation fiberboard with CNFs.

Bending test

Twelve 2.5 by 15.5-cm bending test specimens were cut from two 15.5 by 15.5-cm boards and measured for dimensions and weight. A bending test was performed at a span of 100 mm and a load speed of 3 mm/min with a universal testing machine (BT805/200; Yasui Kikai Co., Ltd, Osaka, Japan). As bending properties, the modulus of rupture (MOR) and modulus of elasticity (MOE) were calculated according to the following equations:

$$\mathrm{MOR} = \frac{3P_{\max}L}{2ah^2} \times 9.81\ (\mathrm{MPa}) \tag{1}$$

$$\mathrm{MOE} = \frac{\Delta P}{\Delta \sigma} \times \frac{L^3}{4ah^3} \times 9.81 \times 10^{-3}\ (\mathrm{GPa}) \tag{2}$$

where $P_{\max}$, L, a, h, P, and σ are breaking weight, span, width, thickness, weight, and displacement, respectively.

Water absorption test

Twelve 25 by 25-mm specimens were prepared from a residual portion of the bending specimen, and the dimensions and weight were measured. Each specimen was immersed for 2 hours in water adjusted to 20°C with a stable low-temperature, high-temperature device (IU800; Yamato Scientific Co., Ltd, Tokyo, Japan). The weight change (WC) and thickness swelling (TS) were calculated according to the following equations:

$$\mathrm{WC} = \frac{W_t - W_0}{W_0} \times 100\ (\%) \tag{3}$$

$$\mathrm{TS} = \frac{T_t - T_0}{T_0} \times 100\ (\%) \tag{4}$$

where W_0, W_t, T_0, and T_t are the initial weight, weight after immersion, initial thickness, and thickness after immersion, respectively.

Thermal conductivity test

Thermal conductivity was measured for three 155 by 155-mm specimens with a thermal conductivity measuring device (HC-074/200; Eko Instruments Co., Ltd, Tokyo, Japan) in accordance with JIS A1412-Part2: Heat Flow Meter Method (Japan Standards Association 1999).

Results and Discussion

Appearance and surface morphology of the IFBs

Figure 2 shows the 0.30-g/cm^3 target density IFB with a CNF addition ratio of 5 wt%. Our lab-scale IFB manufacturing process was able to produce a board with a homogeneous appearance. This result suggests that CNFs can be easily dispersed in IFBs with a stirrer at the mixing stage.

Figure 3 shows SEM images of the surfaces of the 0.30-g/cm^3 target density IFBs with each CNF addition ratio. The wood fiber surfaces of the IFB without CNFs had many voids between the wood fibers. In the case of the IFB with 5% CNFs, a semi-nanofabricated surface structure was observed. The SEM image of this board was magnified to verify the details of CNF absorption on the wood fiber surface (Fig. 4). The CNFs were attached to the surface of the wood fibers. This attachment is mainly due to hydrogen

Figure 2.—The 0.3-g/cm^3 target density insulation fiberboard with a cellulose nanofiber addition ratio of 5 wt%.

bonding (Amini et al. 2017). CNFs have many hydroxyl groups on the surface as a result of being defibrated to nano-order size. It is thought that the hydroxyl groups of the CNFs form many hydrogen bonds between the surfaces of wood fibers, and then the CNF aggregates on the surface when the suspension of CNFs and wood fibers is dried by heat. In the case of the IFB with 10 wt% CNFs (Fig. 3c), some voids between wood fibers were filled by the aggregated CNFs in addition to the CNFs attached to the surfaces of wood fibers. Furthermore, in the case of the IFB with 15 wt% CNFs (Fig. 3d), aggregated CNFs filled almost all voids between the wood fibers. It is thought that the aggregated CNFs filled the voids between the wood fibers because a CNF addition ratio of more than 10 wt% exceeded the maximum amount of CNFs that could be attached to surfaces of wood fibers.

Densities and thicknesses of the IFBs

Table 2 shows the densities and thicknesses of the IFBs with CNFs. For the IFBs with target densities of 0.10 and 0.20 g/cm^3 with CNFs, the actual density of the IFBs was equal to or higher than the target density. For the IFBs with a target density of 0.30 g/cm^3, the actual density was lower than the target density; however, the actual density increased with the CNF addition ratio and approached the target density. On the other hand, the target thickness of any IFB was lower than the actual thickness of the IFB, except for the 0.30-g/cm^3 target density IFBs with 0 and 5 wt% CNFs. With an increase in the CNF addition ratio, the actual board density increased, and the actual thickness decreased. This increase in density was attributable to the decrease in thickness of the boards due to the rise in cohesive force derived from CNF aggregation. Furthermore, it may be related to the higher compressive force from water surface tension caused by the high water retention induced by CNFs. The same phenomena have been reported in the case of surface-fibrillated paper manufactured by beating (Hud-

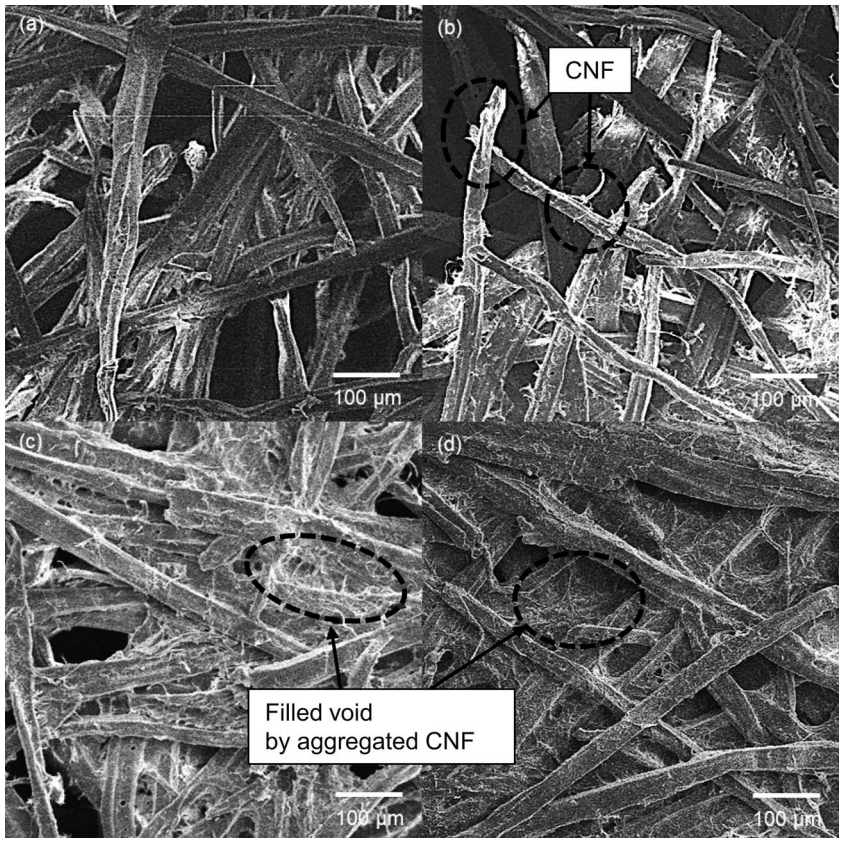

Figure 3.—Scanning electron microscopic images of the surfaces of the 0.30-g/cm^3 target density insulation fiberboard with cellulose nanofiber addition ratios of (a) 0 wt%, (b) 5 wt%, (c) 10 wt%, and (d) 15 wt%.

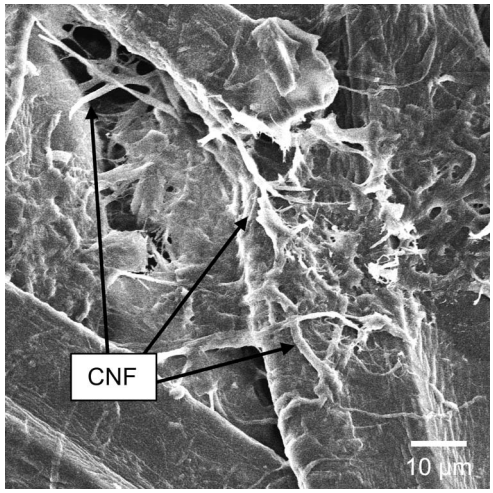

Figure 4.—A highly magnified scanning electron microscopic image of the insulation fiberboard surface (target density of 0.30 g/cm^3 cellulose nanofiber addition ratio of 5 wt%).

son and Cuculo 1980). In a future study, it will be important to develop a method to decrease these forces derived from CNFs in the manufacture of IFBs with CNFs.

Bending properties

Figure 5 shows the bending properties of the IFBs with CNFs. In both MOE and MOR, there were significant difference for the CNF addition ratio, target density, and their interaction with 95 percent confidence level. For any target density IFBs, both the MOR and the MOE values improved with an increasing CNF addition ratio. For example, the MOR and MOE values of all different density IFBs with 15 wt% CNFs were three times higher than those without CNFs. In the case of IFBs without CNFs, the limited contact area between wood fibers resulted in weak chemical bonding (i.e., a small number of hydrogen bonds). By adding CNFs with a significantly higher specific surface area than wood fibers to the IFBs, the fiber contact area was increased. As a result, strong chemical bonding (many hydrogen bonds) occurred. The change in contact area is shown in Figures 3 and 4. Thus, it seems that the bending properties of IFBs increase with a rise in the CNF addition ratio. This conclusion is supported by previous studies on paper (Hubbe 2014, Delgado-Aguilar et al. 2015). In the case of paper, the tensile strength and stiffness increase with an increase in contact area and hydrogen bonding between pulp fibers and CNFs. Additionally, the MORs of the greater than or equal to 0.20-g/cm^3 target density IFBs with CNFs were higher than the standard value of A-class IFBs of JIS A 5905, even though the size of the specimens was different. In addition, the standard deviation of MOR in this study is similar to the previous study (Park et al. 2020), where MOR of IFB with 35 percent resin content was 0.95 $\pm$ 0.1 MPa, whereas in this study, MOR of IFB for 0.07 g/cm^3 with the 15 percent CNF addition ratio was 1.09 $\pm$ 0.19 MPa. This suggests that the IFB with CNF could be produced with same quality as IFB with resin added. Also, the small standard deviation supports the homogeneous distribution of CNF within IFB shown in Figure 2. In the case of MOE, the standard deviation for the same CNF addition ratio did not greatly differ even as the target density increased; that is, standard deviations of MOE for 0.07 and 0.2 g/cm^3 of target density at 10 wt% of the CNF addition ratio were the same as 0.03 MPa. Generally, increasing mechanical properties increases the standard deviation. These phenomena might be caused by filling of the voids with CNF in the board. Although the change in board density and thickness was insufficient, these results suggest that IFBs with CNFs have potential for practical use.

Table 2.—Board density and thickness of insulation fiberboard with cellulose nanofibers (CNFs).[a]

CNF addition ratio (wt%)	Board density (g/cm^3)		Board thickness (mm)	
	Target	Actual	Target	Actual
0	0.07	0.08 (0.01)	10.00	7.88 (0.94)
5		0.09 (0.01)		7.19 (0.91)
10		0.10 (0.00)		6.25 (0.45)
15		0.11 (0.01)		6.09 (0.87)
0	0.10	0.10 (0.00)	10.00	8.86 (0.42)
5		0.11 (0.00)		8.09 (0.27)
10		0.12 (0.00)		7.48 (0.24)
15		0.14 (0.00)		6.82 (0.36)
0	0.20	0.18 (0.00)	10.00	9.91 (0.30)
5		0.20 (0.00)		8.88 (0.36)
10		0.21 (0.00)		8.41 (0.45)
15		0.23 (0.01)		7.76 (0.45)
0	0.30	0.25 (0.02)	10.00	10.73 (0.68)
5		0.26 (0.01)		10.16 (0.51)
10		0.28 (0.01)		9.35 (0.59)
15		0.29 (0.01)		8.88 (0.84)

[a] Actual board density and thickness are shown by average value ($n = 3$). Standard deviations are in parentheses.

Weight changes and thickness swelling

Figure 6 shows the relationship between WC and the target/actual densities of the IFBs with CNFs. In WC, there was a significant difference for the CNF addition ratio, target density, and their interaction at a 95 percent confidence level. The WC of IFB for 0.07 to 0.2 g/cm^3 of target density was almost the same as that for 10 and 15 percent of the CNF addition ratio; however, the WC of other IFBs decreased with an increasing CNF addition ratio (Fig. 6a). It may be attributable to a decrease in the amount of moisture absorbed inside the IFB due to the filling of voids between wood fibers by the aggregated CNFs (see Fig. 3). As shown in Figure 6b, WC decreased as the actual density of the IFBs increased. A strong nonlinear negative correlation was found between WC and the actual density of the IFBs ($R^2 = 0.95$) regardless of the CNF addition ratio.

Figure 7 shows the relationship between TS and the target/actual densities of the IFBs with CNFs. The TS values were significantly different for the CNF addition ratio, target density, and their interaction at a 95 percent confidence level. For the IFBs with a target density of 0.07 g/cm^3 and a CNF addition ratio of 0 percent, the TS was lower than 0 percent. It is thought that fibers are attracted to each other by surface tension when water is removed following the water absorption test in low-density boards. The relationship between TS and actual density showed that TS increased as the actual density of the IFBs increased regardless of the CNF addition ratio (Fig. 7b). The trend of increasing TS with increasing board density generally occurs in wood-

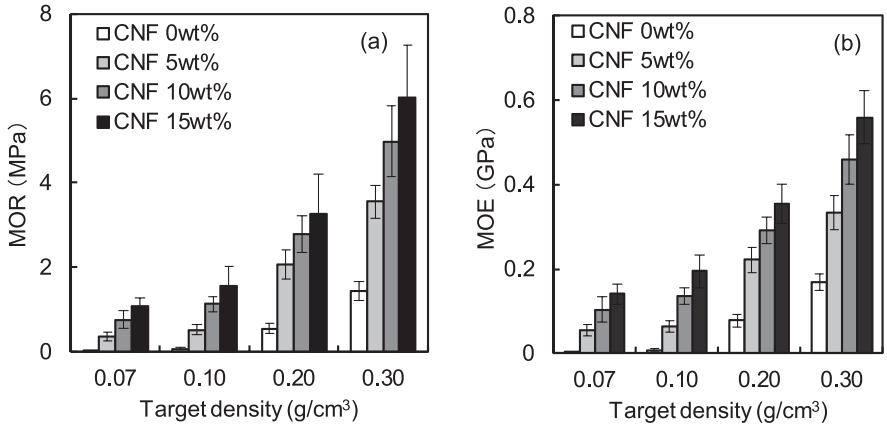

Figure 5.—Bending properties of the insulation fiberboard with cellulose nanofibers: (a) modulus of rupture and (b) modulus of elasticity. The vertical bars indicate standard deviations.

based boards. Furthermore, a nonlinear positive correlation was found between these variables ($R^2 = 0.80$).

In addition, the results showed that TS increased as the CNF addition ratio increased with the exception of IFB for 0.07 g/cm^3 of target density with 10 wt% and 15 wt% of the CNF addition ratio and IFB for 0.3 g/cm^3 of target density with 5 wt% and 10 wt% of the CNF addition ratio. This result may be due to the voids between fibers, which were widened by the decrease in cohesive force attributable to CNFs (i.e., a decrease in the extent of hydrogen bonding). The WC of the IFBs decreased with an increase in the CNF addition ratio (Fig. 6a), although the TS increased. The thickness of the IFBs with CNFs was still lower than the thickness without CNFs after the water absorption test. For example, for the IFBs with a target density of 0.07 g/cm^3, for which a thickness decrement occurred after this test, the actual thicknesses of the IFBs without CNFs and the IFBs with 15 wt% CNFs were about 8.93 and 7.22 mm, respectively. These results suggest that the restraining forces of CNFs (i.e., the cohesive force and the compressive force from water surface tension) remain even after water absorption.

Thermal conductivity

Two-way analysis of variance showed that thermal conductivity was significantly different for the CNF addition ratio, target density, and their interaction at a 95 percent confidence level. Figure 8 shows the relationships between thermal conductivity and actual density of the IFBs with CNFs. Thermal conductivity increased with actual density of the IFBs, and the relationship showed a strong, linear, positive correlation ($R^2 = 0.99$) regardless of the CNF addition ratio. The actual density of the IFBs increased due to a decrease in the voids within the IFBs, and the heat transfer of insulation materials generally increases as solid conduction increases. Therefore, it is thought that the thermal conductivity of the IFBs increased with increasing density because of the effects of void decrease and solid conduction increase. This trend has been observed in many insulation materials (Kawasaki et al. 1998). When the MORs of the IFBs were almost the same, the IFBs with CNFs had lower thermal conductivities than the IFBs without CNFs. For example, the 0 wt% CNF IFBs with the MOR of 1.44 MPa and the 15 wt% CNF IFBs with the MOR of 1.57 MPa had thermal conductivity values of 0.046 and 0.039 W/m·K, respectively. Typically, the mechanical

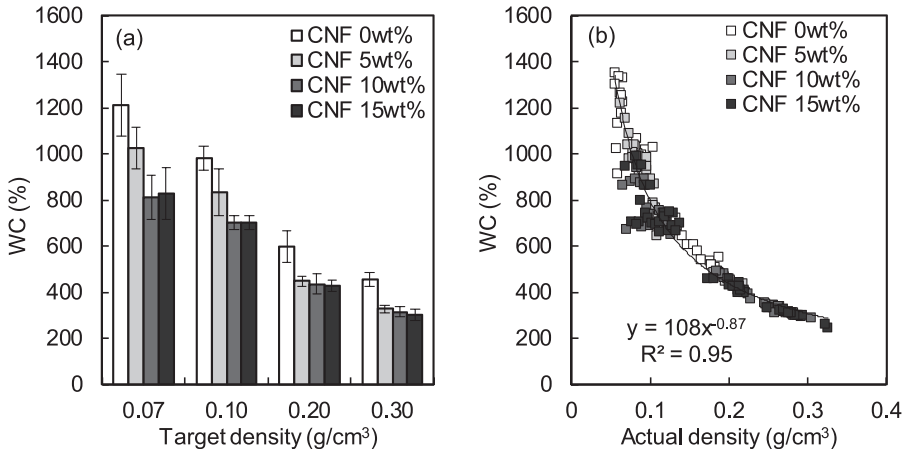

Figure 6.—The relationship between weight change percent (WC%) and (a) target density and (b) actual density of the insulation fiberboard with cellulose nanofibers. The vertical bars in (a) indicate standard deviations. The solid line in (b) represents the power approximation line.

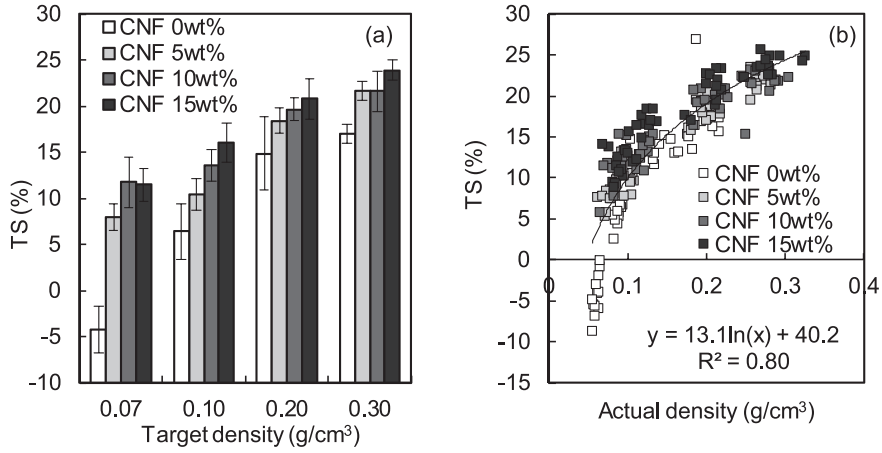

Figure 7.—The relationship between thickness swelling percent (TS%) and (a) target density and (b) actual density of the insulation fiberboard with cellulose nanofibers. The vertical bars in (a) indicate standard deviations. The solid line in (b) represents the logarithmic approximation line.

properties and thermal conductivity increase when the contact area inside an insulation material is higher. In this study, the contact area inside the IFBs was increased by adding CNFs. However, the IFBs with CNFs still had lower thermal conductance than the IFBs without CNFs at the same MOR level. This result suggests that IFBs with the higher MOR and heat insulation performance can be realized by adding CNFs.

Conclusions

This study investigated the lab-scale manufacturing process of IFBs with CNFs and also evaluated the effects of adding CNFs on the physical and mechanical properties of the IFBs. Because the IFBs fabricated with CNFs had a homogeneous appearance, it was assumed that CNFs can be easily dispersed within IFBs during the mixing stage of the wet process of wood-based board production. The actual density, bending properties, and TS of the IFBs with CNFs increased, while the thickness and WC decreased with an increasing CNF addition ratio. As a result of the bending test, the MORs of the greater than or equal to 0.20-g/cm^3 target density IFBs reinforced with CNFs were higher than the standard value of A-class IFBs of JIS A 5905, even though the size of the specimens was different. Furthermore, the actual board density had strong correlations with WC, TS, and thermal conductivity regardless of the CNF addition ratio. In addition, the relationship between MOR and thermal conductivity of the IFBs suggested that IFBs with the higher MOR and heat insulation performance can be realized by adding CNFs. These results suggest that CNF is useful for IFB production as a binder and that fully biomass-derived thermal insulation material will be realized. On the other hand, to produce CNF-reinforced IFBs with the target density and thickness, it is necessary to develop a method for decreasing the cohesive force derived from CNF aggregation and the compressive force originating from the water surface tension caused by the high water retention of CNFs.

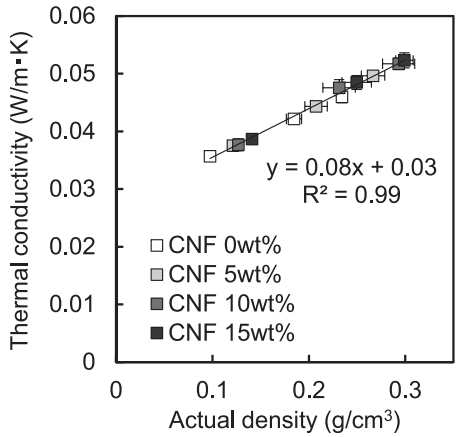

Figure 8.—The relationships between thermal conductivity and actual density of the insulation fiberboard with cellulose nanofibers. The solid line represents the liner approximation line. The vertical bars indicate standard deviations.

Acknowledgment

The authors thank Daiken Corporation for providing the wood fiber used in this study.

Literature Cited

Abe, K., S. Iwamoto, and H. Yano. 2007. Obtaining cellulose nanofibers with uniform width of 0.15 nm from wood. *Biomacromolecules* 8(10):3276–3278.

Amini, E., M. Tajvidi, D. J. Gardner, and D. W. Bousfield. 2017. Utilization of cellulose nanofibrils as a binder for particleboard manufacture. *BioResources* 12(2):4093–4110.

Delgado-Aguilar, M., I. González, M. A. Pèlach, E. De La Fuente, C. Negro, and P. Mutjé. 2015. Improvement of deinked old newspaper/old magazine pulp suspensions by means of nanofibrillated cellulose addition. *Cellulose* 22:789–802.

Hubbe, M. 2014. Prospects for maintaining strength of paper and paperboard products while using less forest resources: A review. *BioResources* 9(1):1634–1763.

Hudson, S. M. and J. A. Cuculo. 1980. The solubility of unmodified cellulose: A critique of the literature. *J. Macromol. Sci. Rev. Macromol. Chem*. 18:1–82.

Ikeda, K., M. Takatani, K. Sakamoto, and T. Okamoto. 2008. Development of fully bio-based composite: Wood/cellulose diacetate/poly(lactic acid) composite. *Holzforschung* 62(2):154–156.

Japanese Standards Association (JSA). 1999. Heat flow meter method. JIS A1412-Part 2. JSA, Tokyo.

Japanese Standards Association (JSA). 2014. Fiberboards. JIS A 5905. JSA, Tokyo.
Kawasaki, T., M. Zhang, and S. Kawai. 1998, Manufacture and properties of ultra-low-density fiberboard. *J. Wood Sci*. 44:354–360.
Kawasaki, M., K. Ishizuka, and K. Kawasaki. 2017. Application to TEMPO-oxidized cellulose nanofiber for the paper product. *Jpn. Tappi* 71:394–398. (In Japanese.)
Kojima, Y., A. Isa, H. Kobori, S. Suzuki, H. Ito, R. Makise, and M. Okamoto. 2014. Evaluation of binding effects in wood flour board containing ligno-cellulose nanofibers. *Materials* 7(9):6853–6864.
Kojima, Y., A. Ishino, H. Kobori, S. Suzuki, H. Ito, R. Makise, I. Higuchi, and M. Okamoto. 2015. Reinforcement of wood flour board containing ligno-cellulose nanofiber made from recycled wood. *J. Wood Sci*. 61(5):492–499.
Kojima, Y., A. Kawabata, H. Kobori, S. Suzuki, H. Ito, R. Makise, and M. Okamoto. 2016. Reinforcement of fiberboard containing ligno-cellulose nanofiber made from wood fibers. *J. Wood Sci*. 62(6):518–525.
Kojima, Y., N. Kato, K. Ota, H. Kobori, S. Suzuki, K. Aoki, and H. Ito. 2018. Cellulose nanofiber as complete natural binder for particleboard. *Forest Prod. J*. 68(3):203–210.
Kondo, T. 2008. New aspects of cellulose nanofiber. *Mokuzai Gakkaishi* 54:107–115. (In Japanese.)
Lee, S. and T. Ohkita. 2003. Mechanical and thermal flow properties of wood flour biodegradable polymer composites. *J. Appl. Polym. Sci*. 90(7):1900–1905.
Park, S-H., M. Lee, P-N. Seo, and E-C. Kang. 2020. Effect of resin content on the physiochemical and combustion properties of wood fiber insulation board. *BioResources* 15(3):5210–5225.
Nakagaito, A. N. and H. Yano. 2005. Novel high-strength biocomposites based on microfibrillated cellulose having nano-order-nit web-like network structure. *Appl. Phys. A* 80(1):155–159.
Okubo, K., T. Fujii, and N. Yamashita. 2005. Improvement of interfacial adhesion in bamboo polymer composite enhanced with microfibrillated cellulose. *JSME Int. J. Ser. A* 48(4):199–204.
Sehaqui, H., M. Allais, Q. Zhou, and L. A. Berglund. 2011. Wood cellulose biocomposites with fibrous structure at micro- and nanoscale. *Compos. Sci. Technol*. 71(3):382–387.
Takatani, M., K. Ikeda, K. Sakamoto, and T. Okamoto. 2008. Cellulose esters as compatibilizers in wood/poly(lactic acid) composite. *J. Wood Sci*. 54(1):54–61.
Umemura, K., O. Sugihara, and S. Kawai. 2013. Investigation of new natural adhesive composed of citric acid and sucrose for particleboard. *J. Wood Sci*. 59(3):203–208.
Umemura, K., T. Ueda, and S. Kawai. 2012a. Characterization of wood-based molding bonded with citric acid. *J. Wood Sci*. 58(1):38–45.
Umemura, K., T. Ueda, and S. Kawai. 2012b. Effects of molding temperature on the physical properties of wood-based molding bonded with citric acid. *Forest Prod. J*. 62(1):63–68.
Umemura, K., T. Ueda, S. S. Munawar, and S. Kawai. 2012c. Application of citric acid as natural adhesive for wood. *J. Appl. Polym. Sci*. 123(4):1991–1996.
Widodo, E., S. S. Kusumah, and K. Umemura. 2020. Development of moulding using sweet sorghum bagasse and citric acid: Effects of application method and citric acid content. *Forest Prod. J*. 70(2):151–157.
Yano, H. 2007. New Developments in Bio-Based Materials. CMC Publishing, Tokyo. (In Japanese.)